First published February 19, 2009; doi:10.1152/japplphysiol.91415.2008.

Ginkgo biloba extract attenuates oxLDL-induced oxidative functional damages in endothelial cells

Hsiu-Chung Ou,[1] Wen-Jane Lee,[2] I-Te Lee,[6] Tsan-Hung Chiu,[3] Kun-Ling Tsai,[4] Chih-Ying Lin,[5] and Wayne Huey-Herng Sheu[6,7,8,9]

[1]*Department of Physical Therapy, College of Health Care, China Medical University, Taichung;* [2]*Department of Education and Medical Research, Taichung Veterans General Hospital, Taichung;* [3]*Department of Obstetrics and Gynecology, China Medical University Hospital, Taichung;* [4]*Graduate Institute of Clinical Medical Science, China Medical University, Taichung;* [5]*Department of Biotechnology, China Medical University, Taichung;* [6]*Division of Endocrinology and Metabolism, Department of Internal Medicine, Taichung Veterans General Hospital, Taichung;* [7]*Institute of Medical Technology, National Chung-Hsing University, Taichung;* [8]*Chung Shan Medical University, Taichung; and* [9]*College of Medicine, National Yang-Ming University, Taipei, Taiwan*

Submitted 24 October 2008; accepted in final form 18 February 2009

Ou HC, Lee WJ, Lee IT, Chiu TH, Tsai KL, Lin CY, Sheu WH. *Ginkgo biloba* extract attenuates oxLDL-induced oxidative functional damages in endothelial cells. *J Appl Physiol* 106: 1674–1685, 2009. First published February 19, 2009; doi:10.1152/japplphysiol.91415.2008.—Atherosclerosis is a chronic inflammatory process with increased oxidative stress in vascular endothelium. *Ginkgo biloba* extract (GbE), extracted from *Ginkgo biloba* leaves, has commonly been used as a therapeutic agent for cardiovascular and neurological disorders. The aim of this study was to investigate how GbE protects vascular endothelial cells against the proatherosclerotic stressor oxidized low-density lipoprotein (oxLDL) in vitro. Human umbilical vein endothelial cells (HUVECs) were incubated with GbE (12.5–100 μg/ml) for 2 h and then incubated with oxLDL (150 μg/ml) for an additional 24 h. Subsequently, reactive oxygen species (ROS) generation, antioxidant enzyme activities, adhesion to monocytes, cell morphology, viability, and several apoptotic indexes were assessed. Our data show that ROS generation is an upstream signal in oxLDL-treated HUVECs. Cu,Zn-SOD, but not Mn-SOD, was inactivated by oxLDL. In addition, oxLDL diminished expression of endothelial NO synthase and enhanced expression of adhesion molecules (ICAM, VCAM, and E-selectin) and the adherence of monocytic THP-1 cells to HUVECs. Furthermore, oxLDL increased intracellular calcium, disturbed the balance of Bcl-2 family proteins, destabilized mitochondrial membrane potential, and triggered subsequent cytochrome *c* release into the cytosol and activation of caspase-3. These detrimental effects were ameliorated dose dependently by GbE ($P < 0.05$). Results from this study may provide insight into a possible molecular mechanism underlying GbE suppression of the oxLDL-mediated vascular endothelial dysfunction.

endothelium; adhesion molecule; apoptosis; reactive oxygen species

ELEVATED LEVELS OF OXIDIZED low-density lipoprotein (oxLDL) are considered to be one of the major risk factors for atherosclerosis and cardiovascular morbidity (49). OxLDL has been detected in atherosclerotic lesions and is thought to play a major role in the initiation and progression of atherosclerosis (55). The morphological changes of cultured endothelial cells associated with oxLDL toxicity are similar to those observed in vivo in endothelial cells covering atherosclerotic areas (41). Reactive oxygen species (ROS) derived from NADPH oxidase have been shown to be strongly associated with atherosclerosis (51). Chen et al. (7) further revealed that oxLDL-induced apoptosis was prevented by radical-scavenging agents and NADPH oxidase inhibitor. The early stages of the atherosclerotic process are initiated by accumulation of oxLDL and activation of endothelial cells with subsequent expression of adhesion molecules and increased binding of monocytes to the vascular endothelium (45). Proinflammatory cytokines, such as IL-1 and TNF-α, which are released when endothelial cells are exposed to oxLDL, upregulate the expression of cell adhesion molecules (39). This series of adverse changes also is associated with a decrease in the bioavailability of nitric oxide (NO), a change that results in a reduced ability of the endothelium to control vessel tone. In addition, oxLDL induces proliferation at lower concentrations and shorter exposure times but induces apoptosis or even necrosis at higher concentrations and longer exposure times (15). It is believed that the induction of apoptosis involves several critical steps, including ROS generation, intracellular calcium accumulation, disturbance of Bcl-2 family protein balance, and reduction of mitochondrial transmembrane potential with concomitant release of mitochondrial protein cytochrome *c* and the subsequent activation of caspase-3 (42).

Ginkgo biloba extract (GbE), a defined complex mixture containing 24% ginkgo flavone glycoside and 6% terpenlactones (ginkgolides, bilobalide), is extracted from the leaves of the *Ginkgo biloba* tree. The flavonoids (ginkgo flavone glycosides, bioflavonoids) and terpenoids (ginkgolides and bilobalide) in GbE have been found to possess antitumor (59), antiaging (12), hepatoprotective (38), and cardioprotective properties (50). It has been used clinically to treat dementia, vaso-occlusive, and cochleovestibular disorders (12, 25). Recent studies have shown that the potential benefits of *Ginkgo biloba* in cardiovascular diseases are mediated through its protective roles against free radical injury. GbE has been shown to inhibit P-selectin-mediated leukocyte adhesion and inflammation (14), scavenge various free radicals (38), increase endothelial NO production, prolong its half-life by the destruction of superoxide radicals on the vascular endothelium (22), and suppress Toll-like receptor 4 expression and NADPH oxidase activation (28).

Although GbE has been shown to have an antioxidant effect both in vivo and in vitro, to the best of our knowledge, there are no studies of these effects on oxLDL-induced endothelial

Address for reprint requests and other correspondence: W. H.-H. Sheu, Division of Endocrinology and Metabolism, Dept. of Internal Medicine, Taichung Veterans General Hospital, No. 160, Sec. 3, Taichung-Kang Road, Taichung 407, Taiwan (e-mail: whhsheu@vghtc.gov.tw).

dysfunction. Therefore, in this study, we tested the hypothesis that GbE could protect against oxLDL-induced endothelial dysfunction by downregulating ROS generation. We undertook the current study to explore the effects of GbE on oxLDL-induced expression of endothelial NO synthase (eNOS) and adhesion molecules and on oxLDL-induced adhesion of monocytes. Furthermore, we also investigated several apoptotic features, such as the accumulation of intracellular calcium and mitochondrial destabilization and the activation of caspase.

MATERIALS AND METHODS

Reagents. Fetal bovine serum (FBS), medium 199 (M199), and trypsin-EDTA were obtained from GIBCO (Grand Island, NY). Low-serum growth supplement (Cascade Biologics, Portland, OR), 2′,7′-bis(2-carboxyethyl)-5(6)-carboxyfluorescein acetoxymethyl ester (BCECF-AM), 4,6-diamidino-2-phenylindole (DAPI), EDTA, penicillin, and streptomycin were obtained from Sigma (St. Louis, MO). GbE, a defined complex mixture containing 24% ginkgo flavone glycoside (primarily composed of quercetin, kaempferol, and isorhamnetin) and 6% terpenlactones (ginkgolides A, B, and C and bilobalide) extracted from *Ginkgo biloba* leaves, was obtained from Dr. Willmar Schwabe (Karlsruhe, Germany). Lactate dehydrogenase (LDH) kits and the terminal deoxynucleotidyl transferase dUTP-mediated nick-end labeling (TUNEL) staining kit were obtained from Boehringer Mannheim (Mannheim, Germany). The superoxide dismutase activity assay kit was purchased from Calbiochem (San Diego, CA). Dihydroethidium (DHE) and the EnzChek caspase-3 assay kit were purchased from Molecular Probes (Eugene, OR). 5,58,6,68-tetraethylbenzimidazolcarbocyanine iodide (JC-1) and anti-active caspase 3 were obtained from BioVision (Palo Alto, CA). Anti-vascular cell adhesion molecule-1 (VCAM-1), anti-intercellular adhesion molecule (ICAM), and anti-E-selectin were purchased from R&D Systems (Minneapolis, MN). Anti-Cu,Zn superoxide dismutase (SOD-1) and anti-Mn superoxide dismutase (SOD-2) were obtained from Santa Cruz Biotechnology (Santa Cruz, CA). Anti-eNOS, anti-Bcl-2, and anti-Bax were obtained from BD Transduction Laboratories (San Diego, CA).

Cell cultures. This experiment was approved by the Research Ethics Committee of Taichung Veterans General Hospital. With the written consent of the parents, fresh human umbilical cords were obtained after birth, collected, and suspended in Hanks' balanced salt solution (GIBCO) at 4°C. Human umbilical vein endothelial cells (HUVECs) were isolated from human umbilical cord with collagenase and used at *passages 2* and *3* (19). After dissociation, the cells were collected and cultured on gelatin-coated culture dishes in M199 with low-serum growth supplement, 100 IU/ml penicillin, and 0.1 mg/ml streptomycin. Subcultures were performed with trypsin-EDTA. Media were refreshed on every second day. The identity of umbilical vein endothelial cells was confirmed by their cobblestone morphology and strong positive immunoreactivity to von Willebrand factor. THP-1, a human monocytic leukemia cell line, was obtained from American Type Culture Collection (Rockville, MD) and cultured in RPMI with 10% FBS at a density of 2–5 $\times$ 10^6 cells/ml as suggested in the product specification sheet provided by the manufacturer.

Lipoprotein separation. Human plasma was obtained from the Taichung Blood Bank, and LDL was isolated using sequential ultracentrifugation (ρ = 1.019–1.210 g/ml) in KBr solutions containing 30 mM EDTA, stored at 4°C in a sterile, dark environment, and used within 3 days (17). Immediately before the oxidation tests, LDL was separated from EDTA and from diffusible low-molecular mass compounds by gel filtration on PD-10 Sephadex G-25 M gel (Pharmacia) in 0.01 M phosphate-buffered saline (136.9 mM NaCl, 2.68 mM KCl, 4 mM Na_2HPO_4, and 1.76 mM KH_2PO_4, pH 7.4). Cu^{2+}-modified LDL (1 mg protein/ml) was prepared by exposing LDL to 10 μM $CuSO_4$ for 16 h at 37°C. Protein was measured by the method used by Bradford (4).

Measurement of ROS production. ROS, such as superoxide (O_2^-) and hydrogen peroxide (H_2O_2), are specific mediators of atherogenic stimuli that induce leukocyte adhesion to endothelial cells. In addition, the role that ROS plays in oxLDL-mediated cytotoxicity is believed to be through the induction of apoptosis and the activation of the caspase cascade (18). The effect of GbE on ROS production in HUVECs was determined by performing a fluorometric assay using DHE as a probe for the presence of superoxide. After preincubation for 2 h with the indicated concentrations of GbE, HUVECs were incubated with DHE for 1 h, followed by incubation with oxLDL for the indicated time periods. The fluorescence intensity was measured at 540-nm excitation and 590-nm emission using a Labsystems fluorescence microplate reader. The percent increase in fluorescence per well was calculated using the formula $[(Ft_2 - Ft_0)/Ft_0] \times 100$, where Ft_2 is the fluorescence at 2 h of oxLDL exposure and Ft_0 is the fluorescence at 0 min of oxLDL exposure.

Measurement of SOD activity. To determine the effect of GbE on antioxidant enzyme after oxLDL treatment, SOD activity in the homogenate was determined by an enzymatic assay method using a commercial kit (Calbiochem) according to the manufacturer's instructions. Enzyme activity was converted to units per milligram of protein.

Immunoblotting. To determine whether GbE could ameliorate the oxLDL-diminished SOD-1, SOD-2, eNOS, Bcl-2, and Bax protein expression, HUVECs were grown to confluence, pretreated with GbE for 2 h, and then stimulated with oxLDL for 24 h. At the end of stimulation, cells were washed, scraped from dishes, and lysed in RIPA buffer (in mM: 20 HEPES, 1.5 $MgCl_2$, 2 EDTA, 5 EGTA, 0.1 DTT, and 0.1 PMSF, pH 7.5). Proteins (30 μg) were then separated by electrophoresis on SDS-polyacrylamide gel. After the proteins had been transferred onto a polyvinylidene difluoride membrane (Millipore, Bedford, MA), the blot was incubated with blocking buffer (1$\times$ PBS and 5% nonfat dry milk) for 1 h at room temperature and then probed with primary antibodies (SOD-1, SOD-2, eNOS, Bcl-2, Bax; 1:1,000 dilutions) overnight at 4°C, followed by incubation with horseradish peroxidase-conjugated secondary antibody (1:5,000) for 1 h. To control equal loading of total protein in all lanes, blots were stained with mouse anti-β-actin antibody at a 1:50,000 dilution. The bound immunoproteins were detected by an enhanced chemiluminescence assay (ECL; Amersham, Little Chalfont, UK), and the intensities were quantified by densitometric analysis (Digital Protein DNA Imagineware, Huntington Station, NY).

Adhesion assay. HUVECs at 1 $\times$ 10^5 cells/ml were cultured in 96-well flat-bottom plates (0.1 ml/well) for 1–2 days. Cells were then pretreated with the indicated concentrations of GbE for 2 h and incubated with oxLDL (150 μg/ml) for 24 h. The medium was then removed, and 0.1 ml/well of THP-1 cells (prelabeled with 4 μM BCECF-AM for 30 min in RPMI at a 1 $\times$ 10^6 cell/ml density) was added in RPMI. The cells were allowed to adhere at 37°C for 1 h in a 5% CO_2 incubator. The nonadherent cells were removed by gentle aspiration. Plates were washed three times with M199. The number of adherent cells was estimated by microscopic examination; the cells were then lysed with 0.1 ml of 0.25% Triton X-100. The fluorescence intensity was measured at 485-nm excitation and 538-nm emission using a Labsystems fluorescence microplate reader.

Adhesion molecule expression. To determine whether GbE could modify the oxLDL-induced adhesion molecule expression, HUVECs were grown to confluence, pretreated with GbE for 2 h, and stimulated with oxLDL (150 μg/ml) for 24 h. At the end of stimulation, HUVECs were harvested and incubated with FITC-conjugated anti-VCAM-1, anti-ICAM-1, and anti-E-selectin (R&D Systems) for 45 min at room temperature. After the HUVECs had been washed three times, their immunofluorescence intensity was analyzed by flow

cytometry using a Becton Dickinson FACScan flow cytometer (Mountain View, CA).

Measurement of intracellular calcium. To determine the effect of GbE on the rise of oxLDL-induced intracellular calcium level ($[Ca^{2+}]_i$), HUVECs were seeded onto 24-mm glass coverslips, pretreated with GbE for 2 h, and then stimulated with oxLDL (150 μg/ml) for the indicated time periods. The cells on the coverslips were loaded with 2 μM fura-2 AM (Molecular Probes) in M199 and allowed to stand for 30 min at 37°C. After loading, the cells were washed with HEPES buffer (in mM: 131 NaCl, 5 KCl, 1.3 $CaCl_2$, 1.3 Mg_2SO_4, 0.4 KH_2PO_4, 20 HEPES, and 25 glucose, pH 7.4) to remove excess fluorescent dye. The fluorescence of the cells on each coverslip was then measured and recorded using an inverted Olympus IX-70 microscope. $[Ca^{2+}]_i$ in endothelial cells was monitored at an emission wavelength of 510 nm with excitation wavelengths alternating between 340 and 380 nm with the use of a Delta Scan System (Photon Technology International, Princeton, NJ) and calculated using the method of Grynkiewicz et al. (16).

Measurement of mitochondrial membrane potential. The lipophilic cationic probe fluorochrome JC-1 was used to explore the effect of GbE on the mitochondrial membrane potential ($\Delta\Psi_m$). JC-1 exists as either a green fluorescent monomer at depolarized membrane potentials or a red fluorescent J-aggregate at hyperpolarized membrane potentials. JC-1 exhibits potential-dependent accumulation in mitochondria, as indicated by the fluorescence emission shift from 530 to 590 nm. After cells were treated with oxLDL (150 μg/ml) for 24 h in the presence or absence of various concentrations of GbE, cells (5×10^4 cells/24-well plate) were rinsed with M199, and JC-1 (5 μM) was loaded. After 20 min of incubation at 37°C, cells were examined under a fluorescence microscope. Determination of the $\Delta\Psi_m$ was carried out using a FACScan flow cytometer (3).

Isolation of cytosolic fraction for cytochrome c analysis. After cells were treated with oxLDL in the presence and absence of GbE, the cells were collected and lysed with lysis buffer (20 mM HEPES-NaOH, pH 7.5, 250 mM sucrose, 10 mM KCl, 2 mM $MgCl_2$, 1 mM EDTA, 1 mM DTT, and protease inhibitor cocktail) for 20 min on ice. The samples were homogenized by 10 passages through a 2-gauge needle. The homogenate was then centrifuged at 12,000 rpm for 20 min at 4°C. Protein was measured using the Bradford method (4). A volume of cell lysates containing 30 μg of protein was analyzed by Western blot analysis for cytochrome *c* (1:1,000) and β-actin (1:50,000).

Measurement of active caspase-3. To explore the effect of GbE on oxLDL-induced caspase-3 activation, HUVECs were pretreated with GbE for 2 h and then stimulated with oxLDL (150 μg/ml) for 24 h. The level of active caspase-3 was detected by flow cytometry using a commercial fluorescein active caspase kit (Mountain View, CA) (48) and a fluorescence microscope. Activity of caspase-3 also was measured using the EnzChek caspase-3 assay kit according to the manufacturer's instructions (Molecular Probes). After being lysed by repeated freeze-thaw, cells were incubated on ice for 15 min and centrifuged at 15,000 *g* for 20 min. The protein concentrations of the supernatants were determined. Equal amounts of protein (50 μg) were added to the reaction buffer containing 5 mM of caspase-3 substrate Z-DEVD-R110, and the mixture was incubated at room temperature for 30 min. The fluorescence generated from cleavage of the substrate by caspase-3 was monitored with a Labsystems fluorescence microplate reader at excitation and emission wavelengths of 496 and 520 nm, respectively.

Determination of cytotoxicity and indexes of apoptosis. To determine the effect of GbE on oxLDL-induced cytotoxicity, HUVECs were first incubated with GbE for 2 h and then stimulated with oxidized LDL for 24 h. At the end of stimulation, mitochondrial dehydrogenase activity, which can be used as an index of cell viability, was assessed using the 3-(4,5-dimethylthiazol-2-yl)-2,5-diphenyltetrazolium (MTT) assay (11). Plasma membrane integrity was assessed by measuring LDH release using an LDH diagnostic kit according to the manufacturer's instructions. Apoptotic cells were

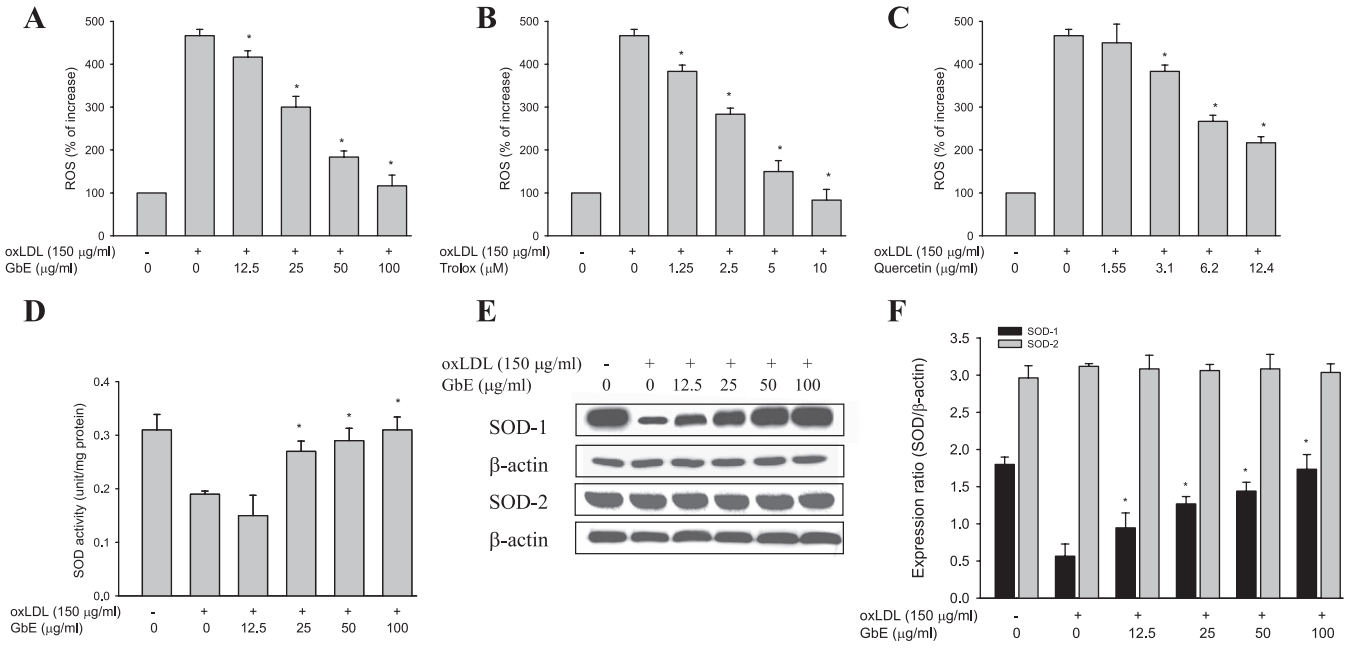

Fig. 1. Inhibitory effects of *Ginkgo biloba* extract (GbE) on oxidized low-density lipoprotein (oxLDL)-induced reactive oxygen species (ROS) production in human umbilical vein endothelial cells (HUVECs). After preincubation for 2 h with 12.5–100 μg/ml GbE (*A*), 1.25–10 μM Trolox (*B*), and 1.55–12.4 μg/ml quercetin (*C*), 150 μg/ml oxLDL was added to the medium for 2 h, followed by a 1-h incubation with the fluorescent probe dihydroethidium (DHE; 10 μM). Fluorescence intensity of cells was measured with a fluorescence microplate reader. Fluorescence distribution of DHE oxidation was expressed as a percentage of increased intensity. *D*: the activities of SOD in HUVECs stimulated with oxLDL in the absence or presence of GbE were determined. *E* and *F*: representative Western blots of Cu,Zn-superoxide dismutase (SOD-1) and Mn-SOD (SOD-2) protein levels in HUVECs pretreated with GbE for 2 h, followed by 150 μg/ml oxLDL for 24 h (E). Densitometric data are means ± SE of 3 independent analyses (F). *$P < 0.05$ compared with oxLDL-stimulated HUVECs.

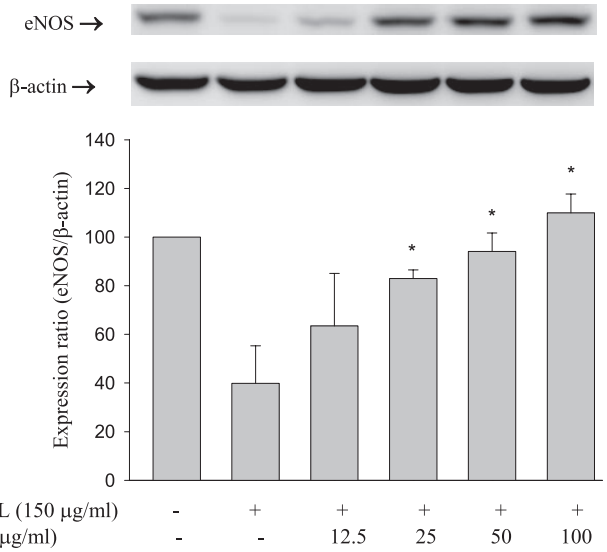

Fig. 2. Effects of GbE on oxLDL-impaired endothelial nitric oxide synthase (eNOS) protein expression. HUVECs were pretreated for 2 h with indicated concentrations of GbE, followed by 150 μg/ml oxLDL for 24 h. For Western blot analyses, a monoclonal anti-eNOS and a monoclonal anti-β-actin antibody (for normalization) were used. Values are means ± SE of 3 independent analyses. *$P < 0.05$ vs. oxLDL treatment.

assessed by a TUNEL assay under a fluorescence microscope or in a flow cytometer.

Statistical analyses. Results are means ± SE, and data were analyzed using one-way ANOVA followed by Student's *t*-test for significant difference. A P value <0.05 was considered statistically significant.

RESULTS

GbE inhibited oxLDL-induced ROS generation in HUVECs. A previous study demonstrated that oxLDL evoked a progressive rise in cellular ROS, which subsequently led to the activation of apoptotic signaling (43). We therefore investigated the effects of GbE on the generation of ROS, a potential factor related to oxLDL-induced endothelial cell injury, by using DHE. Pretreatment of HUVECs with GbE (12.5–100 μg/ml) for 2 h before exposure to 150 μg/ml oxLDL significantly decreased the level of ROS generation in a dose-dependent manner (all $P < 0.05$) (Fig. 1*A*). Preincubation of HUVECs with Trolox (a potent antioxidant as a positive control) similarly inhibited ROS generation caused by oxLDL (Fig. 1*B*). The maximal inhibitory effect was achieved at 100 μg/ml in GbE (95.6% inhibition, $P < 0.05$) and at 10 μM in Trolox (104% inhibition, $P < 0.05$), respectively. Since GbE contains 24% ginkgo flavone glycoside, and its anti-inflammatory and antioxidant activities depend on its various components, such as quercetin, kaempferol, and isorhamnetin, all of which have been used in previous studies with different effects (2, 9), we decided to compare the efficacy of quercetin (a main flavonoid component in GbE) and GbE on modulation of ROS reduction. Our results suggested that quercetin at the concentrations of 1.55, 3.1, 6.2, and 12.4 μg/ml, similar to that contained in 12.5, 25, 50, and 100 μg/ml GbE, was not as potent as GbE in ROS reduction (Fig. 1*C*). Thus we believe that quercetin probably is not the sole component responsible for the in vitro inhibition of oxLDL-induced ROS generation by GbE.

Intracellular ROS levels are regulated by the balance between ROS generation and antioxidant enzymes. In addition, the involved ROS are able to inactivate antioxidative enzymes that additionally increase the imbalance in favor of oxidative stress. We next turned our attention to the total activity of SOD and the expression of its isoforms in endothelial cells in response to oxLDL. Our results showed that GbE at concentrations >25 μg/ml significantly reduced the suppression of SOD activity caused by oxLDL (Fig. 1*D*). SOD-1, but not SOD-2, expression was diminished after treatment with oxLDL for 24 h and could be significantly rescued by pretreatment with GbE (Fig. 1, *E* and *F*).

GbE ameliorated oxLDL-diminished eNOS protein expression. OxLDL has been shown to reduce the release of NO from endothelial cells, thereby causing endothelial dysfunction (37). It also has been shown that GbE increases eNOS expression (22). In this study, we examined whether GbE could rescue eNOS protein expression after treatment with oxLDL. As

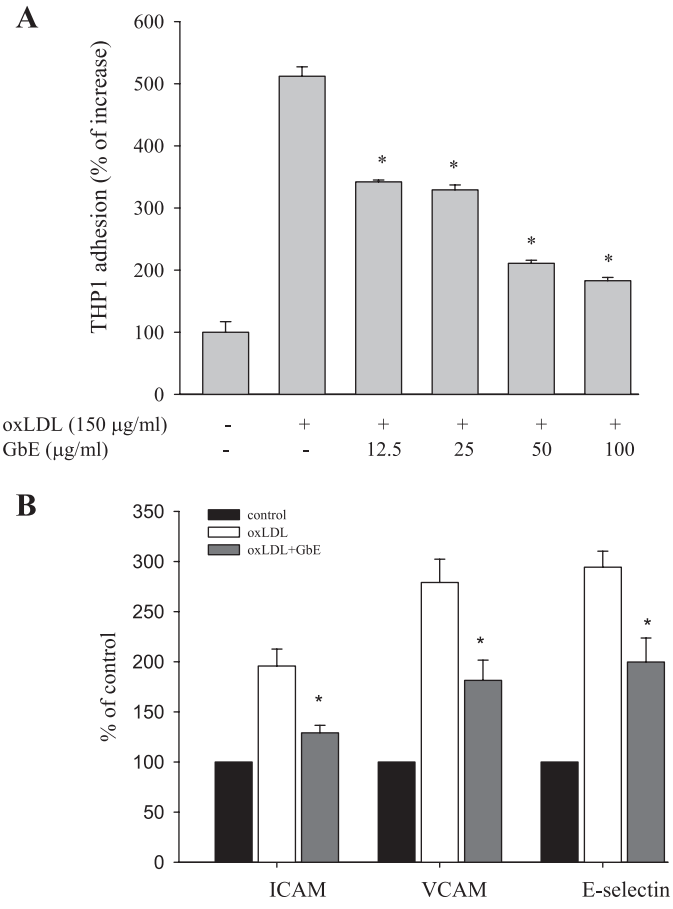

Fig. 3. Effects of GbE on oxLDL-induced adhesiveness of HUVECs to THP-1 monocytic cells and adhesion molecule expression. Cells were incubated with indicated concentrations of GbE for 2 h and then incubated with ox-LDL for an additional 24 h. *A*: dose-dependent effect of GbE (12.5–100 μg/ml) on oxLDL (150 μg/ml)-induced adhesiveness of HUVECs to THP-1 was measured as described in MATERIALS AND METHODS. Values are means ± SE from 4 separate experiments. *$P < 0.05$ vs. oxLDL treatment. *B*: HUVECs were incubated with oxLDL (150 μg protein/ml) in the absence (control) or presence (oxLDL + GbE) of 50 μg/ml GbE for 24 h. The histogram of cell surface expression of VCAM-1, ICAM-1, and E-selectin was generated by flow cytometry. Values are means ± SE of 3 independent analyses. *$P < 0.05$ vs. oxLDL treatment.

shown in Fig. 2, oxLDL significantly reduced eNOS protein expression in HUVECs after 24 h of incubation (39.9%, $P < 0.05$); however, this tendency was reversed significantly with GbE pretreatment.

GbE suppressed oxLDL-induced adherence of THP-1 cells to HUVECs and expression of adhesion molecules. OxLDL-enhanced recruitment, retention, and adhesiveness of human monocytes and monocytic cell lines to endothelium have been implicated in the initial stage of atherogenesis (21). To test the effect of GbE on monocyte adhesion to HUVECs, confluent monolayers of HUVECs were pretreated with various concentrations of GbE for 2 h and then stimulated with oxLDL (150 μg/ml) for 24 h, followed by incubation with THP-1 cells for 1 h at 37°C. As shown in Fig. 3*A*, oxLDL stimulated an increase in adherence of THP-1 cells to HUVECs (512 ± 15%, $P < 0.05$); however, the effect was significantly inhibited by GbE treatment in a dose-dependent manner (all $P < 0.05$). The effect of GbE on the surface expression of adhesion molecules on HUVECs exposed to oxLDL was subsequently examined. As shown in Fig. 3*B*, the expression levels of VCAM-1, ICAM-1, and E-selectin were significantly higher in HUVECs that had been treated with oxLDL (150 μg/ml) for 24 h than in the control cells (195, 279, and 294%, respectively, compared with control). Flow cytometry revealed that the induction of adhesion molecule expression was significantly ameliorated by the presence of 50 μg/ml GbE (all $P < 0.05$).

GbE reduced oxLDL-induced intracellular Ca^{2+} accumulation. To investigate the effect of chronic exposure of endothelial cells to a cytotoxic concentration of oxLDL on intracellular calcium, we incubated HUVECs with oxLDL (150 μg/ml) in the absence or presence of GbE. As shown in Fig. 4, the basal level of $[Ca^{2+}]_i$ increased in oxLDL-treated cells after 24 h, whereas GbE significantly inhibited the oxLDL-enhanced intracellular calcium rise (all $P < 0.05$).

Effect of GbE on mitochondrial transmembrane permeability transition. Because high cytosolic calcium levels can theoretically activate several proapoptotic mechanisms mediated by calcium-dependent enzymes, mitochondrial permeability transition pore opening, or calcium-induced osmotic swelling/rupture of mitochondrial membranes (52), it was of interest to identify the calcium-dependent apoptotic pathways. To examine whether inhibition of mitochondrial disruption accounts for the antiapoptotic effect of GbE, we tested the effects of oxLDL on mitochondrial permeability. When HUVECs were exposed to oxLDL (150 μg/ml), the $\Delta\Psi_m$ was depolarized, as shown by the increase in green fluorescence (Fig. 5*A*, *middle*). Pretreatment with GbE reduced the change in $\Delta\Psi_m$, as indicated by repression of green fluorescence and restoration of red fluorescence (Fig. 5*A*, *right*). Quantitative analysis from flow cytometry supported these findings. As shown in Fig. 5*B*, oxLDL caused a marked increase in JC-1 green fluorescence (*middle*) compared with the control (*left*). Pretreatment with GbE caused marked inhibition of this oxLDL-induced apoptotic index (Fig. 5*B*, *right*).

GbE mitigated the proapoptotic effects of oxLDL on Bcl-2 family proteins, mitochondrial cytochrome c release, and caspase-3 activation. Bcl-2 family proteins are upstream regulators of mitochondrial membrane potential. Since oxLDL

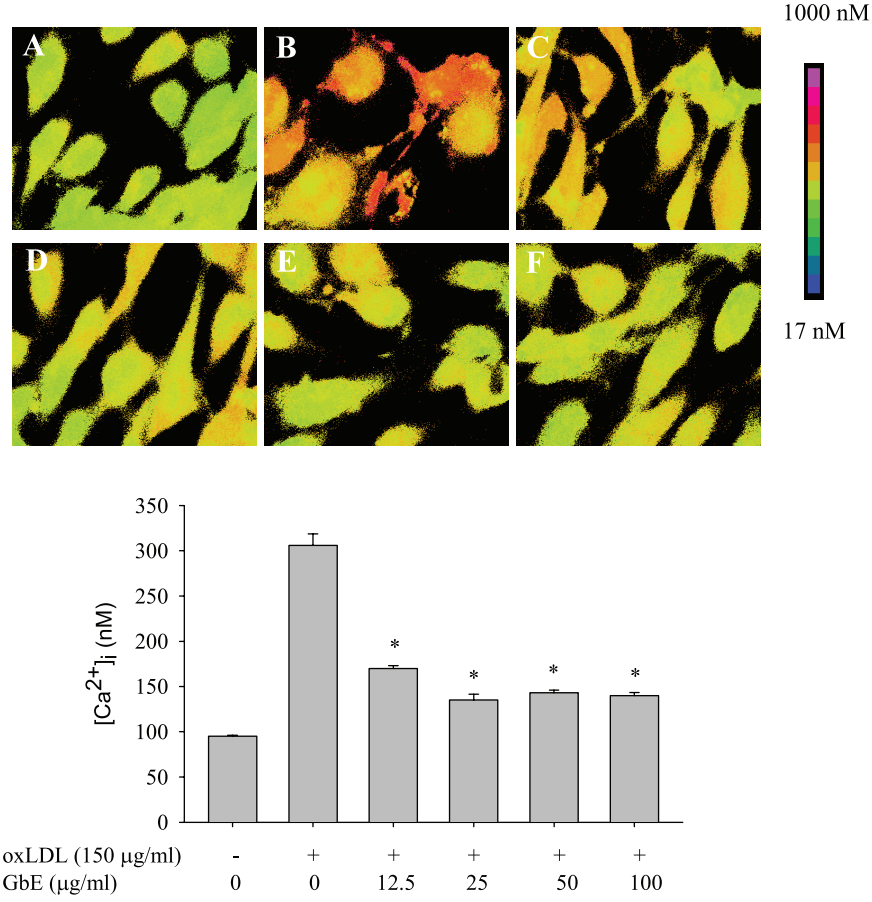

Fig. 4. Effects of GbE on the oxLDL-induced increase in cytoplasmic Ca^{2+} levels ($[Ca^{2+}]_i$) in fura-2-loaded HUVECs. Cells were incubated with indicated concentrations of GbE for 2 h and then incubated with 150 μg/ml oxLDL for an additional 24 h. Images were processed as indicated in MATERIALS AND METHODS. Ca^{2+} changes are color coded (see color bar at *right*) such that warm colors indicate high $[Ca^{2+}]_i$. *A*: no treatment. *B*: oxLDL. *C*: oxLDL + 12.5 μg/ml GbE. *D*: oxLDL + 25 μg/ml GbE. *E*: oxLDL + 50 μg/ml GbE. *F*: oxLDL + 100 μg/ml GbE. Values represent means ± SE of more than 250 individual cells from 3 separate experiments. *$P < 0.05$ vs. oxLDL treatment.

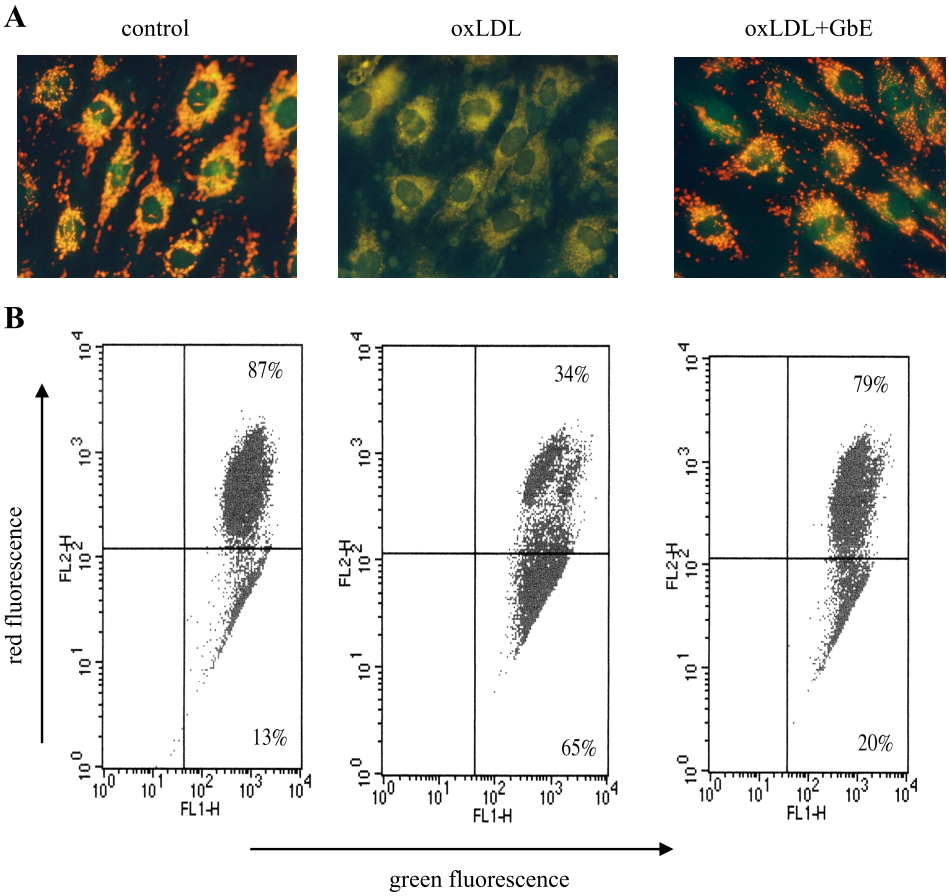

Fig. 5. Effects of GbE on mitochondrial transmembrane permeability transition. Cells were incubated with 50 μg/ml GbE for 2 h and then incubated with 150 μg/ml oxLDL for an additional 24 h. *A*: the change in mitochondrial membrane potential was assessed based on the signal intensity from monomeric and J-aggregate JC-1 fluorescence as described in MATERIALS AND METHODS. *Left*, no treatment; *middle*, oxLDL; *right*, oxLDL + GbE. *B*: JC-1 fluorescence was confirmed by flow cytometry. Green fluorescence intensity indicates the cells with low $\Delta\Psi_m$, while the red fluorescence intensity indicated the cells with stable $\Delta\Psi_m$. Data show a representative experiment from a minimum of 3 independent experiments.

depolarized $\Delta\Psi_m$ whereas GbE maintained it, whether GbE also influenced the equilibrium of Bcl-2 family proteins was investigated. Immunoblotting studies demonstrated that oxLDL downregulated the antiapoptotic (Bcl-2) and upregulated the proapoptotic (Bax) proteins, whereas GbE pretreatment effectively repressed these oxLDL-evoked proapoptotic events (Fig. 6*A*). Quantitative analysis ascertained that oxLDL significantly decreased the Bcl-2-to-Bax ratio, but GbE pretreatment preserved this antiapoptotic index (Fig. 6*A*, bar graph).

It is known that disruption of mitochondrial membrane function results in the specific release of the mitochondrial enzyme cytochrome *c* into the cytosol. Therefore, mitochondria were separated from the cytosolic fraction and detected by Western blotting. As shown in Fig. 6*B*, the amount of cytochrome *c* released into the cytosolic fraction was much greater in HUVECs that had been incubated with oxLDL for 24 h than in control cells. The results indicate that GbE significantly prevented oxLDL-induced release of cytochrome *c*.

Caspase-3 is a key factor in the execution of mitochondrial apoptosis (52). To examine whether oxLDL and GbE ultimately influence this factor to modulate apoptosis, we subsequently determined the active form of caspase-3 by using fluorescence microscopy and flow cytometry. As shown in Fig. 7*A*, active caspase-3 was significantly increased in cells that had been treated with oxLDL for 24 h. In contrast, the activation of caspase-3 by oxLDL was suppressed in cells that had been pretreated with 50 μg/ml GbE. The activity of caspase-3 was confirmed using the EnzChek caspase-3 assay kit. The results showed that oxLDL significantly upregulated caspase-3 activity 3.1-fold, whereas GbE pretreatment effectively suppressed the activity of this apoptotic factor, implying a stimulatory effect of oxLDL and inhibitory action of GbE on caspase-3 activity.

GbE inhibited oxLDL-induced cytotoxicity of HUVECs. Phase-contrast microscopy was performed to examine the protective effects of GbE on morphological features of HUVECs after exposure to oxLDL. After a 24-h exposure to oxLDL, the number of shrunken cells or cells with blebbing membranes was significantly reduced by the presence of GbE (Fig. 8*A*). The viability of cells incubated with oxLDL in the absence or presence of indicated concentrations of GbE was assessed using the MTT assay, and membrane permeability was assayed by LDH release. Our results showed that oxLDL significantly reduced viability and increased membrane permeability in HUVECs after 24 h of incubation (50 and 399% compared with control, respectively); however, pretreatment with GbE inhibited oxLDL-induced cytotoxicity of HUVECs dose dependently (all $P < 0.05$).

GbE inhibited oxLDL-induced apoptosis of HUVECs. To further ascertain whether cell death induced by oxLDL was an apoptotic event in HUVECs, oxLDL-treated cells were analyzed biochemically via TUNEL and DAPI staining assays and evaluated by microscopic observation and flow cytometry. As shown in Fig. 9, cells incubated with oxLDL for 24 h showed typical features of apoptosis, including the formation of condensed nuclei, which were, however, not observed in the GbE-pretreated HUVECs. As described above, cell viability assay coupled with phenotypic observation of apoptosis under

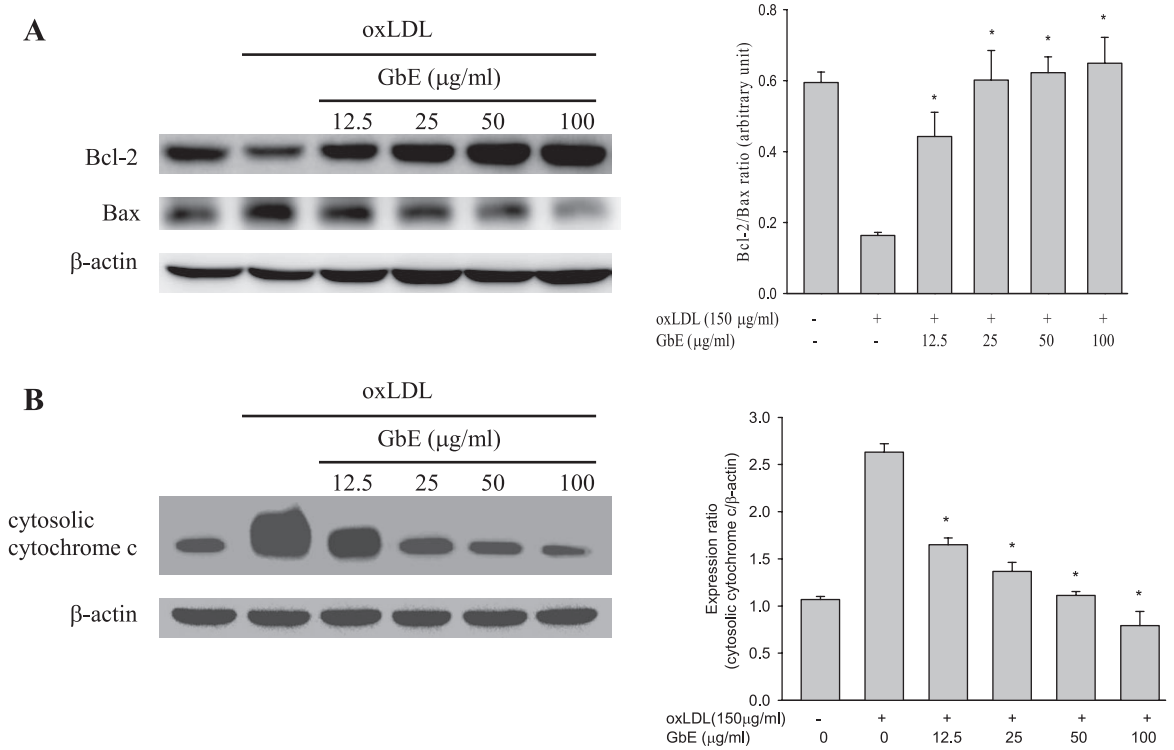

Fig. 6. Immunoblotting analysis of Bcl-2 family proteins (*A*) and mitochondrial cytochrome *c* release (*B*) in response to oxLDL and GbE. HUVECs were incubated with 150 μg/ml oxLDL in the absence or presence of indicated concentrations (12.5–100 μg/ml) of GbE for 24 h. Representative Western blots (*left*) and summary data (*right*) show that oxLDL upregulated proapoptotic (Bax) and downregulated antiapoptotic (Bcl-2) proteins and increased the abundance of cytochrome *c* in the cytosolic fraction, whereas GbE pretreatment suppressed these apoptosis-provoking alterations. Results of densitometric analysis are means ± SE of 3 separate experiments. $^*P < 0.05$ vs. oxLDL treatment.

microscopy and flow cytometry suggested that GbE is a potent inhibitor of oxLDL-induced cytotoxicity in cultured HUVECs.

DISCUSSION

There is a growing body of evidence, ranging from in vitro experiments to pathological analyses and epidemiological studies, which indicates the beneficial role of GbE in the treatment of cardiovascular disease (35, 36); however, its clinical use is still underrepresented because of the lack of knowledge about its cellular and molecular mechanisms of action (60). The aim of the present study was to elucidate the underlying mechanism by which GbE protects against oxLDL-induced endothelial dysfunction. The main findings of this study indicate that the pretreatment with GbE significantly suppressed the oxLDL-induced endothelial dysfunction in cultured HUVECs. Of particular interest is the findings that the protective effects of GbE resulted from decreased ROS generation that subsequently attenuated the oxLDL-impaired antioxidant activities and increased the bioavailability of NO, the maintenance of endothelial $[Ca^{2+}]_i$, and the stabilization of mitochondria, thereby preventing the release of mitochondrial protein cytochrome *c*, a molecule required for the activation of caspase-3 that executes the cell death program.

Since GbE is a complex mixture of ingredients with a unique broad spectrum of pharmacological activities, it probably acts through several different mechanisms covering ROS scavenger and enhancing SOD activities. For example, it is a potent superoxide anion scavenger with SOD activities (40). It also directly activates SOD activity/synthesis toward reducing free radical formation and stabilizing membranes rather than scavenging free radicals (44). Previous studies have demonstrated that endothelial dysfunction caused by oxLDL is due to a decrease in antioxidative enzymes (26), thereby inducing apoptosis by activating multiple ROS-sensitive signaling pathways (29). In addition, treatment with GbE led to a significant enhancement of cellular SOD activities in keratinocytes (61) and cardiomyocytes (44). ROS generated by endothelial cells include O_2^-, H_2O_2, peroxynitrite (·ONOO), NO, and hydroxyl (·OH) radicals (27). The major source of ROS in endothelial cells is the NADPH oxidase system (1). Intracellular ROS levels are regulated by the balance between ROS-generating enzymes and antioxidant enzymes that include SOD, catalase, and glutathione peroxidase. Blood vessels express three isoforms of SOD, namely, cytosolic or Cu, Zn-SOD (SOD-1), Mn-SOD (SOD-2) localized in mitochondria, and an extracellular form of Cu,Zn-SOD (EC-SOD; SOD-3) (13). SOD protects against superoxide-mediated cytotoxicity by catalyzing O_2^- to form H_2O_2. Cu,Zn-SOD, but not Mn-SOD, inactivated by H_2O_2 produced from superoxide anion (20), plays a key role in atherosclerosis (53). An increase in activity of Cu,Zn-SOD prevents oxLDL-induced endothelial dysfunction (47). A previous study demonstrated that GbE exhibits an activity similar to that of Cu,Zn-SOD; for example, 75 μg/ml GbE possesses an activity equal to that observed with 0.22 U Fridovich of bovine Cu,Zn-SOD (40), and a cDNA microarray study (46) showed that RNA expression of Cu,Zn-SOD,

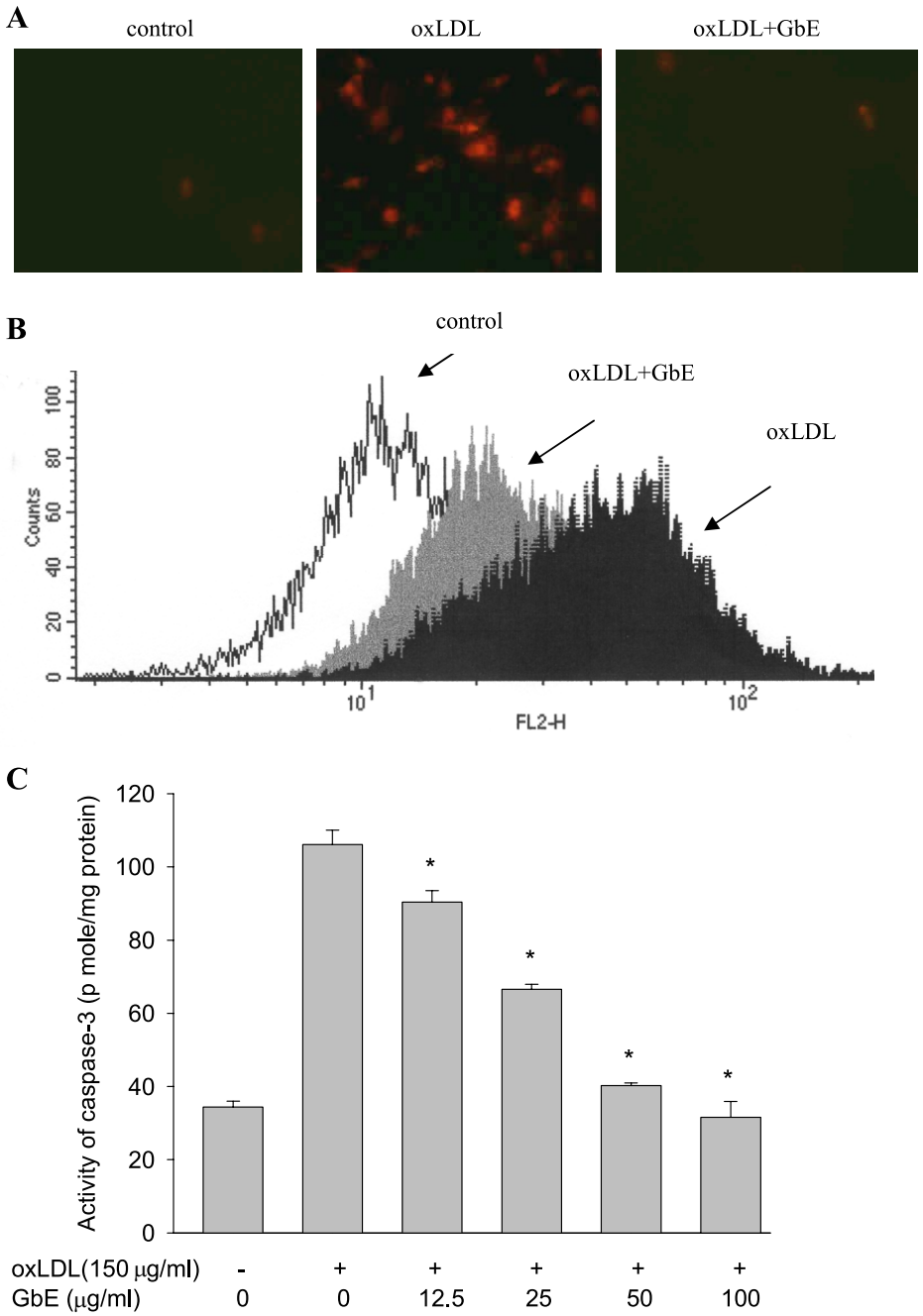

Fig. 7. Effects of GbE on oxLDL-induced caspase-3 activation. HUVECs were incubated with oxLDL in the absence or presence of indicated concentrations of GbE for 24 h. *A*: fluorescence images show the activated caspase-3 level in control cells (*left*), HUVECs stimulated with oxLDL (*middle*), and in the presence of GbE (*right*). *B*: fluorescence intensity of cells was measured with flow cytometry. *C*: the activity of caspase-3 was 3.1-fold higher in oxLDL-treated HUVECs compared with the control but was limited to a 2.6- to 0.9-fold increase when pretreated with GbE (12.5–100 μg/ml). Values are means ± SE of 3 independent analyses. $*P < 0.05$ vs. oxLDL treatment.

but not Mn-SOD, was increased by GbE. In accordance with these studies, our results showed that GbE treatment significantly reduced ROS generation that subsequently ameliorated oxLDL-attenuated SOD-1 expression. We assume that the mechanisms by which GbE protects against oxLDL-induced endothelial dysfunction could be mainly through the ROS scavenger with SOD activity.

In many vascular pathologies, a combination of altered rates of NO production along with an increased removal of NO leads to an apparent reduction in the bioavailability of NO. The antithrombotic and antiatherosclerotic properties of NO are achieved by its ability to inhibit the expression of the cell surface adhesion molecules P-selectin, VCAM, and ICAM (23), prevent the expression of monocyte chemoattractant protein (MCP)-1 (57), and inhibit platelet adhesion under flow conditions (10). In normal physiology, superoxide is detoxified by the enzyme SOD, thereby preventing its interaction with NO. Our data show that GbE ameliorated the oxLDL-diminished expression of eNOS and had an inhibitory effect on the oxLDL-induced adhesiveness between monocytes and HUVECs. We further examined the inhibitory effects of GbE on the oxLDL-induced surface expression of adhesion molecules in HUVECs. As expected, GbE repressed the oxLDL-induced surface expression of these adhesion molecules. All of these findings strongly indicate the antioxidative and anti-inflammatory effects of GbE in response to oxLDL treatment in HUVECs. Our findings support those of previous reports that demonstrated

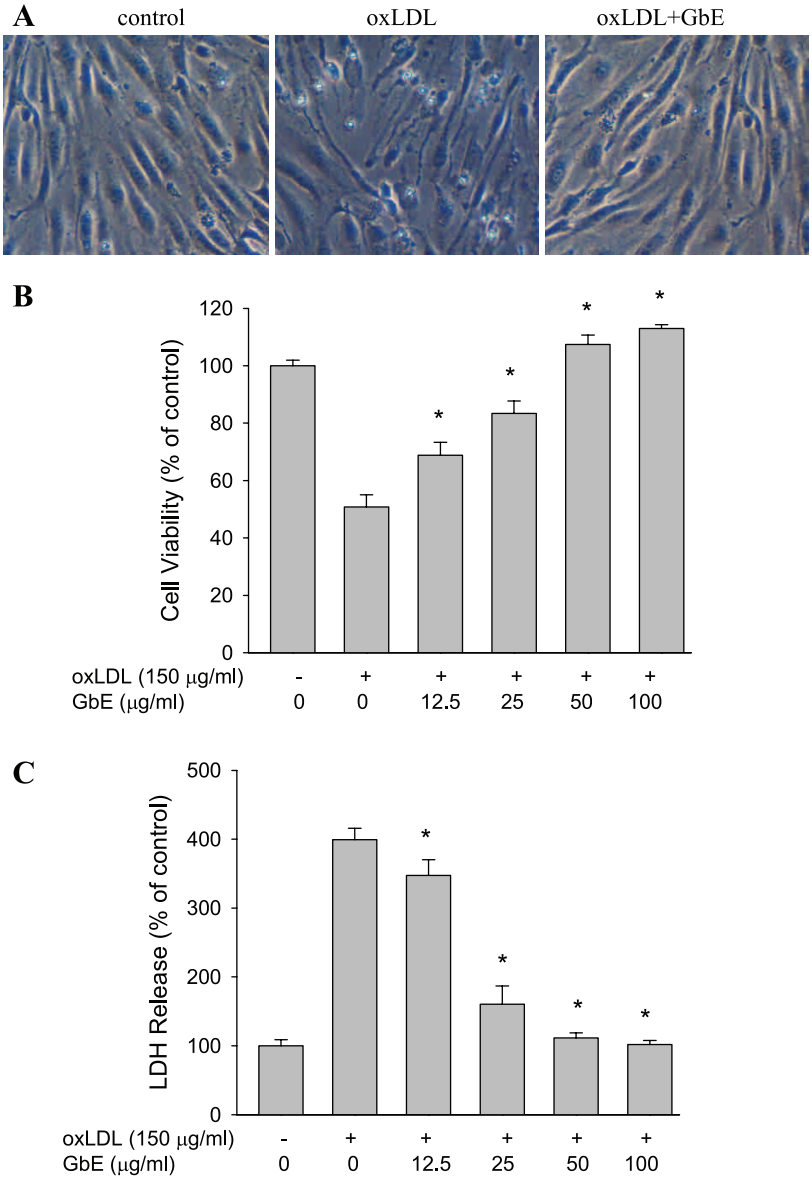

Fig. 8. Effects of GbE on oxLDL-induced endothelial cell death. *A*: HUVECs were incubated with oxLDL (150 μg protein/ml) in the absence (*middle*) or presence (*right*) of various concentrations of GbE for 24 h. Photomicrographs are from phase-contrast microscopy. Viability was determined via MTT assay (*B*) and lactate dehydrogenase (LDH) release (*C*). Values are means ± SE of 3 separate experiments. *$P < 0.05$ vs. oxLDL treatment.

the antioxidative effects of GbE derived from inhibition of ROS production via suppression of NADPH oxidase activation (28) and the sphingomyelinase ceramide pathway (31). With regard to the underlying mechanisms of anti-inflammation, GbE inhibits P-selectin-mediated leukocyte adhesion and inflammation (14) and acts as a potent inhibitor of NF-κB, a key transcription factor in the expression of inflammatory cytokines (6). In addition, recent studies have shown that ginkgo improves endothelium-dependent vasodilation (54) and reduces doxorubicin-induced apoptotic damage in rat hearts and neonatal cardiomyocytes (32). Together, these findings suggest that GbE might be a candidate drug for the prevention of cardiovascular diseases.

Although modulation of biological signaling pathways by ROS depends on both the upstream ligand-dependent stimulation of ROS production and the specific interactions of ROS with individual downstream pathways, NADPH oxidases seem to be especially important in that they are the main source whose primary function appears to be to modulate redox signaling (5). OxLDL rapidly elevates ROS and then multiple downstream events are activated via secondary messengers, including p38 mitogen-activated protein kinase (MAPK) or phosphoinositide 3-kinase (PI3K), both causing NF-κB activation and enabling nuclear translocation and subsequent regulation of proinflammatory gene expression (8). In the present study, GbE at a dose as low as 50 μg/ml was sensitive enough to reverse the inhibitory effect on SOD and eNOS expression but only partially effective in reducing adhesion molecule expression and monocytic adherence. We assumed that GbE at this dose might not be able to abolish completely all of the ROS that were generated when exposed to oxLDL and/or other downstream pathways involved that together led to partial inhibition of adhesion molecule expression.

Pathophysiological stimuli that induce endothelial activation via NADPH oxidase-mediated ROS-induced signal transduction and alteration of intracellular Ca^{2+} ion homeostasis are now considered to be major contributors to the

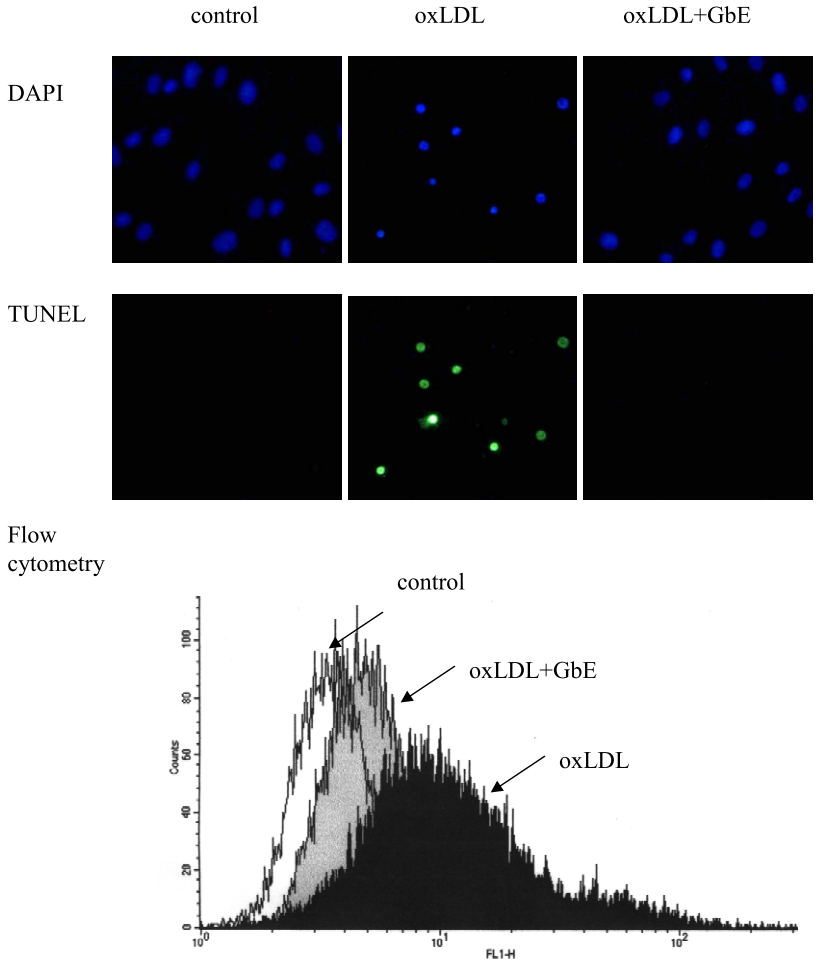

Fig. 9. Effects of GbE on oxLDL-induced endothelial cell apoptosis. HUVECs were incubated with oxLDL (150 μg protein/ml) in the absence (*middle* images) or presence (*right* images) of 50 μg/ml GbE for 24 h. *Top* images show cells stained with 4,6-diamidino-2-phenylindole (DAPI); *bottom* images show cells stained using terminal deoxynucleotidyl transferase dUTP-mediated nick-end labeling (TUNEL) assay. Arrows indicate condensed nuclei. Graph displays flow cytometric analysis. Data show a representative experiment from a minimum of 3 independent experiments.

atherosclerotic coronary artery diseases (33). Endothelial cells do not possess voltage-operated L-type calcium channels. Matsui et al. (34) demonstrated that nifedipine, a calcium channel blocker, decreased advanced glycation end product-induced MCP-1 overexpression by inhibiting ROS generation and subsequent NF-κB activation via suppression of NADPH oxidase. Our study found that ROS generation was the earliest apoptotic signal and that it usually occurred within 5 min after the addition of oxLDL. Therefore, we assume that the antiapoptotic effects of GbE were due to its ability to decrease the level of ROS generation, which helped maintain the level of mitochondrial $[Ca^{2+}]_i$ in endothelial cells, thereby preventing the release of mitochondrial protein cytochrome *c*, a molecule required for the activation of caspase-3. In addition, the oxLDL-induced increase in ROS preceded the increase in $[Ca^{2+}]_i$ (2 vs. 24 h), suggesting that the increase in $[Ca^{2+}]_i$ induced by oxidative stress may be a consequence of free radical action on calcium ions stored in intracellular organelles. Our finding that GbE reduced the level of apoptosis and cell death is especially relevant because increased endothelial cell apoptosis may initiate atherosclerotic lesions (30). Whether inhibition of NADPH oxidase is involved in the effect of GbE on oxLDL-induced ROS generation requires further study.

The concentrations of GbE required to suppress the oxLDL-induced endothelial dysfunction in our study were similar to those reported to inhibit other responses, such as smooth muscle cell proliferation, vascular endothelial growth factor, thrombomodulin expression, and tissue-type plasminogen activator secretion (24, 28, 58). The dose of GbE used in previous in vitro studies, which usually ranged from 200 to 400 μg/ml, seems to be relatively high compared with the dose used in the current study. The recommended dose of GbE injection is 87.5 mg/day for patients with chronic vascular disease (56). In humans, it is unclear how much the circulating blood level would be elevated by a single dose of GbE, since the pharmacokinetics of the components of GbE have not been completely established. It also is unknown whether prolonged use of GbE would lead to chronic accumulation of some of the components in different tissues.

In summary, the results from our experiments indicate that GbE attenuates oxLDL-induced oxidative functional damages in endothelial cells, probably via its antioxidative and anti-inflammatory functions, by reducing the oxLDL-induced ROS generation and impairment of antioxidant enzymes, the expression of adhesion molecules, and the adhesiveness between monocytes and HUVECs. In addition, GbE inhibited oxLDL-induced cell death and apoptosis in HUVECs. Our work adds GbE to the growing list of herbal remedies whose mode of action has been at least partially revealed on a molecular level.

GRANTS

This study was supported by National Science Council Grants NSC 96-2320-B-039-040 and NSC 95-2314-B-075A-020-MY3, China Medical University Grant CMU-96-118, and Taichung Veterans General Hospital Grant 973001C (Taiwan, Republic of China).

REFERENCES

1. **Babior BM.** The NADPH oxidase of endothelial cells. *IUBMB Life* 50: 267–269, 2000.
2. **Bao M, Lou Y.** Isorhamnetin prevents endothelial cell injuries from oxidized LDL via activation of p38MAPK. *Eur J Pharmacol* 547: 22–30, 2006.
3. **Bedner E, Li X, Gorczyca W, Melamed MR, Darzynkiewicz Z.** Analysis of apoptosis by laser scanning cytometry. *Cytometry* 35: 181–195, 1999.
4. **Bradford MM.** A rapid and sensitive method for the quantitation of microgram quantities of protein utilizing the principle of protein-dye binding. *Anal Biochem* 72: 248–254, 1976.
5. **Cai H, Griendling KK, Harrison DG.** The vascular NAD(P)H oxidases as therapeutic targets in cardiovascular diseases. *Trends Pharmacol Sci* 24: 471–478, 2003.
6. **Chen JW, Chen YH, Lin FY, Chen YL, Lin SJ.** *Ginkgo biloba* extract inhibits tumor necrosis factor-α-induced reactive oxygen species generation, transcription factor activation, and cell adhesion molecule expression in human aortic endothelial cells. *Arterioscler Thromb Vasc Biol* 23: 1559–1566, 2003.
7. **Chen XP, Xun KL, Wu Q, Zhang TT, Shi JS, Du GH.** Oxidized low density lipoprotein receptor-1 mediates oxidized low density lipoprotein-induced apoptosis in human umbilical vein endothelial cells: role of reactive oxygen species. *Vascul Pharmacol* 47: 1–9, 2007.
8. **Chen XP, Zhang TT, Du GH.** Lectin-like oxidized low-density lipoprotein receptor-1, a new promising target for the therapy of atherosclerosis? *Cardiovasc Drug Rev* 25: 146–161, 2007.
9. **Crespo I, Garcia-Mediavilla MV, Gutierrez B, Sanchez-Campos S, Tunon MJ, Gonzalez-Gallego J.** A comparison of the effects of kaempferol and quercetin on cytokine-induced pro-inflammatory status of cultured human endothelial cells. *Br J Nutr* 100: 968–976, 2008.
10. **De Graaf JC, Banga JD, Moncada S, Palmer RM, de Groot PG, Sixma JJ.** Nitric oxide functions as an inhibitor of platelet adhesion under flow conditions. *Circulation* 85: 2284–2290, 1992.
11. **Denizot F, Lang R.** Rapid colorimetric assay for cell growth and survival. Modifications to the tetrazolium dye procedure giving improved sensitivity and reliability. *J Immunol Methods* 89: 271–277, 1986.
12. **Diamond BJ, Shiflett SC, Feiwel N, Matheis RJ, Noskin O, Richards JA, Schoenberger NE.** *Ginkgo biloba* extract: mechanisms and clinical indications. *Arch Phys Med Rehabil* 81: 668–678, 2000.
13. **Faraci FM, Didion SP.** Vascular protection: superoxide dismutase isoforms in the vessel wall. *Arterioscler Thromb Vasc Biol* 24: 1367–1373, 2004.
14. **Fei R, Fei Y, Zheng S, Gao YG, Sun HX, Zeng XL.** Purified polysaccharide from *Ginkgo biloba* leaves inhibits P-selectin-mediated leukocyte adhesion and inflammation. *Acta Pharmacol Sin* 29: 499–506, 2008.
15. **Galle J, Heinloth A, Wanner C, Heermeier K.** Dual effect of oxidized LDL on cell cycle in human endothelial cells through oxidative stress. *Kidney Int Suppl* 78: S120–S123, 2001.
16. **Grynkiewicz G, Poenie M, Tsien RY.** A new generation of Ca^{2+} indicators with greatly improved fluorescence properties. *J Biol Chem* 260: 3440–3450, 1985.
17. **Havel RJ, Eder HA, Bragdon JH.** The distribution and chemical composition of ultracentrifugally separated lipoproteins in human serum. *J Clin Invest* 34: 1345–1353, 1955.
18. **Hsieh CC, Yen MH, Yen CH, Lau YT.** Oxidized low density lipoprotein induces apoptosis via generation of reactive oxygen species in vascular smooth muscle cells. *Cardiovasc Res* 49: 135–145, 2001.
19. **Jaffe EA, Nachman RL, Becker CG, Minick CR.** Culture of human endothelial cells derived from umbilical veins. Identification by morphologic and immunologic criteria. *J Clin Invest* 52: 2745–2756, 1973.
20. **Jewett SL, Rocklin AM, Ghanevati M, Abel JM, Marach JA.** A new look at a time-worn system: oxidation of CuZn-SOD by H_2O_2. *Free Radic Biol Med* 26: 905–918, 1999.
21. **Kim JA, Territo MC, Wayner E, Carlos TM, Parhami F, Smith CW, Haberland ME, Fogelman AM, Berliner JA.** Partial characterization of leukocyte binding molecules on endothelial cells induced by minimally oxidized LDL. *Arterioscler Thromb* 14: 427–433, 1994.
22. **Koltermann A, Hartkorn A, Koch E, Furst R, Vollmar AM, Zahler S.** *Ginkgo biloba* extract EGb 761 increases endothelial nitric oxide production in vitro and in vivo. *Cell Mol Life Sci* 64: 1715–1722, 2007.
23. **Kubes P, Suzuki M, Granger DN.** Nitric oxide: an endogenous modulator of leukocyte adhesion. *Proc Natl Acad Sci USA* 88: 4651–4655, 1991.
24. **Lan WJ, Zheng XX.** Activity of *Ginkgo biloba* extract and quercetin on thrombomodulin expression and tissue-type plasminogen activator secretion by human umbilical vein endothelial cells. *Biomed Environ Sci* 19: 249–253, 2006.
25. **Le Bars PL, Katz MM, Berman N, Itil TM, Freedman AM, Schatzberg AF.** A placebo-controlled, double-blind, randomized trial of an extract of *Ginkgo biloba* for dementia. North American EGb Study Group. *JAMA* 278: 1327–1332, 1997.
26. **Li D, Yang B, Mehta JL.** Ox-LDL induces apoptosis in human coronary artery endothelial cells: role of PKC, PTK, bcl-2, and Fas. *Am J Physiol Heart Circ Physiol* 275: H568–H576, 1998.
27. **Li JM, Shah AM.** Endothelial cell superoxide generation: regulation and relevance for cardiovascular pathophysiology. *Am J Physiol Regul Integr Comp Physiol* 287: R1014–R1030, 2004.
28. **Lin FY, Chen YH, Chen YL, Wu TC, Li CY, Chen JW, Lin SJ.** *Ginkgo biloba* extract inhibits endotoxin-induced human aortic smooth muscle cell proliferation via suppression of Toll-like receptor 4 expression and NADPH oxidase activation. *J Agric Food Chem* 55: 1977–1984, 2007.
29. **Lin SJ, Shyue SK, Liu PL, Chen YH, Ku HH, Chen JW, Tam KB, Chen YL.** Adenovirus-mediated overexpression of catalase attenuates oxLDL-induced apoptosis in human aortic endothelial cells via AP-1 and C-Jun N-terminal kinase/extracellular signal-regulated kinase mitogen-activated protein kinase pathways. *J Mol Cell Cardiol* 36: 129–139, 2004.
30. **Littlewood TD, Bennett MR.** Apoptotic cell death in atherosclerosis. *Curr Opin Lipidol* 14: 469–475, 2003.
31. **Liu KX, He W, Rinne T, Liu Y, Zhao MQ, Wu WK.** The effect of *Ginkgo biloba* extract (EGb 761) pretreatment on intestinal epithelial apoptosis induced by intestinal ischemia/reperfusion in rats: role of ceramide. *Am J Chin Med* 35: 805–819, 2007.
32. **Liu TJ, Yeh YC, Ting CT, Lee WL, Wang LC, Lee HW, Wang KY, Lai HC, Lai HC.** *Ginkgo biloba* extract 761 reduces doxorubicin-induced apoptotic damage in rat hearts and neonatal cardiomyocytes. *Cardiovasc Res* 80: 227–235, 2008.
33. **Madamanchi NR, Vendrov A, Runge MS.** Oxidative stress and vascular disease. *Arterioscler Thromb Vasc Biol* 25: 29–38, 2005.
34. **Matsui T, Yamagishi S, Nakamura K, Inoue H, Takeuchi M.** Nifedipine, a calcium-channel blocker, inhibits advanced glycation end-product-induced expression of monocyte chemoattractant protein-1 in human cultured mesangial cells. *J Int Med Res* 35: 107–112, 2007.
35. **Morgenstern C, Biermann E.** The efficacy of *Ginkgo* special extract EGb 761 in patients with tinnitus. *Int J Clin Pharmacol Ther* 40: 188–197, 2002.
36. **Muir AH, Robb R, McLaren M, Daly F, Belch JJ.** The use of *Ginkgo biloba* in Raynaud's disease: a double-blind placebo-controlled trial. *Vasc Med* 7: 265–267, 2002.
37. **Mukherjee S, Coaxum SD, Maleque M, Das SK.** Effects of oxidized low-density lipoprotein on nitric oxide synthetase and protein kinase C activities in bovine endothelial cells. *Cell Mol Biol (Noisy-le-grand)* 47: 1051–1058, 2001.
38. **Naik SR, Panda VS.** Antioxidant and hepatoprotective effects of *Ginkgo biloba* phytosomes in carbon tetrachloride-induced liver injury in rodents. *Liver Int* 27: 393–399, 2007.
39. **Ohta H, Wada H, Niwa T, Kirii H, Iwamoto N, Fujii H, Saito K, Sekikawa K, Seishima M.** Disruption of tumor necrosis factor-alpha gene diminishes the development of atherosclerosis in ApoE-deficient mice. *Atherosclerosis* 180: 11–17, 2005.
40. **Pincemail J, Dupuis M, Nasr C, Hans P, Haag-Berrurier M, Anton R, Deby C.** Superoxide anion scavenging effect and superoxide dismutase activity of *Ginkgo biloba* extract. *Experientia* 45: 708–712, 1989.
41. **Ross R.** The pathogenesis of atherosclerosis: a perspective for the 1990s. *Nature* 362: 801–809, 1993.
42. **Salvayre R, Auge N, Benoist H, Negre-Salvayre A.** Oxidized low-density lipoprotein-induced apoptosis. *Biochim Biophys Acta* 1585: 213–221, 2002.
43. **Schmitt A, Salvayre R, Delchambre J, Negre-Salvayre A.** Prevention by alpha-tocopherol and rutin of glutathione and ATP depletion induced by oxidized LDL in cultured endothelial cells. *Br J Pharmacol* 116: 1985–1990, 1995.

44. **Schneider R, Welt K, Aust W, Loster H, Fitzl G.** Cardiac ischemia and reperfusion in spontaneously diabetic rats with and without application of EGb 761. I. Cardiomyocytes. *Histol Histopathol* 23: 807–817, 2008.
45. **Sigurdardottir V, Fagerberg B, Hulthe J.** Circulating oxidized low-density lipoprotein (LDL) is associated with risk factors of the metabolic syndrome and LDL size in clinically healthy 58-year-old men (AIR study). *J Intern Med* 252: 440–447, 2002.
46. **Soulie C, Nicole A, Christen Y, Ceballos-Picot I.** The *Ginkgo biloba* extract EGb 761 increases viability of hnt human neurons in culture and affects the expression of genes implicated in the stress response. *Cell Mol Biol (Noisy-le-grand)* 48: 641–646, 2002.
47. **Tang F, Wu X, Wang T, Wang P, Li R, Zhang H, Gao J, Chen S, Bao L, Huang H, Liu P.** Tanshinone II A attenuates atherosclerotic calcification in a rat model by inhibition of oxidative stress. *Vascul Pharmacol* 46: 427–438, 2007.
48. **Telford WG, Komoriya A, Packard BZ.** Detection of localized caspase activity in early apoptotic cells by laser scanning cytometry. *Cytometry* 47: 81–88, 2002.
49. **Toshima SI, Hasegawa A, Kurabayashi M, Itabe H, Takano T, Sugano J, Shimamura K, Kimura J, Michishita I, Suzuki T, Nagai R.** Circulating oxidized low density lipoprotein levels: a biochemical risk marker for coronary heart disease. *Arterioscler Thromb Vasc Biol* 20: 2243–2247, 2000.
50. **Tunali-Akbay T, Sener G, Salvarli H, Sehirli O, Yarat A.** Protective effects of *Ginkgo biloba* extract against mercury(II)-induced cardiovascular oxidative damage in rats. *Phytother Res* 21: 26–31, 2007.
51. **Vendrov AE, Madamanchi NR, Hakim ZS, Rojas M, Runge MS.** Thrombin and NAD(P)H oxidase-mediated regulation of CD44 and BMP4-Id pathway in VSMC, restenosis, and atherosclerosis. *Circ Res* 98: 1254–1263, 2006.
52. **Vindis C, Elbaz M, Escargueil-Blanc I, Auge N, Heniquez A, Thiers JC, Negre-Salvayre A, Salvayre R.** Two distinct calcium-dependent mitochondrial pathways are involved in oxidized LDL-induced apoptosis. *Arterioscler Thromb Vasc Biol* 25: 639–645, 2005.
53. **Vora DK, Fang ZT, Liva SM, Tyner TR, Parhami F, Watson AD, Drake TA, Territo MC, Berliner JA.** Induction of P-selectin by oxidized lipoproteins: separate effects on synthesis and surface expression. *Circ Res* 80: 810–818, 1997.
54. **Wu Y, Li S, Cui W, Zu X, Du J, Wang F.** *Ginkgo biloba* extract improves coronary blood flow in healthy elderly adults: role of endothelium-dependent vasodilation. *Phytomedicine* 15: 164–169, 2008.
55. **Yla-Herttuala S, Palinski W, Rosenfeld ME, Steinberg D, Witztum JL.** Lipoproteins in normal and atherosclerotic aorta. *Eur Heart J* 11, *Suppl* E: 88–99, 1990.
56. **Wu YZ, Li SQ, Zu XG, Du J, Wang FF.** *Ginkgo biloba* extract improves coronary artery circulation in patients with coronary artery disease: contribution of plasma nitric oxide and endothelin-1. *Phytother Res* 22: 734–739, 2008.
57. **Zeiher AM, Fisslthaler B, Schray-Utz B, Busse R.** Nitric oxide modulates the expression of monocyte chemoattractant protein-1 in cultured human endothelial cells. *Circ Res* 76: 980–986, 1995.
58. **Zhang L, Rui YC, Yang PY, Qiu Y, Li TJ, Liu HC.** Inhibitory effects of *Ginkgo biloba* extract on vascular endothelial growth factor in rat aortic endothelial cells. *Acta Pharmacol Sin* 23: 919–923, 2002.
59. **Zhang Y, Chen AY, Li M, Chen C, Yao Q.** *Ginkgo biloba* extract kaempferol inhibits cell proliferation and induces apoptosis in pancreatic cancer cells. *J Surg Res* 148: 17–23, 2008.
60. **Zhou W, Chai H, Lin PH, Lumsden AB, Yao Q, Chen C.** Clinical use and molecular mechanisms of action of extract of *Ginkgo biloba* leaves in cardiovascular diseases. *Cardiovasc Drug Rev* 22: 309–319, 2004.
61. **Zhu QX, Shen T, Tu DY, Ding R, Liang ZZ, Zhang XJ.** Protective effects of *Ginkgo biloba* leaf extracts on trichloroethylene-induced human keratinocyte cytotoxicity and apoptosis. *Skin Pharmacol Physiol* 18: 160–169, 2005.